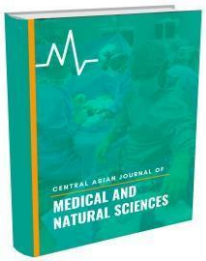

CENTRAL ASIAN JOURNAL OF MEDICAL AND NATURAL SCIENCES
https://cajmns.centralasianstudies.org/index.php/CAJMNS
Volume: 06 Issue: 04 | October 2025 ISSN: 2660-4159

Article

Electrical and Structural Properties of $Hg_1Ba_2Ca_2Cu_3O_{8+\delta}$ Superconductor Synthesized via Solid-State Reaction at Different Sintering Temperatures

Ahmed Majid Safi*[1], Sabah Jalal Fathi[2]

1,2. Department of Physics, College of Education for Pure Science, University of Kirkuk, Iraq
* Correspondence: ephm23010@uokirkuk.edu.iq

Abstract: High-temperature superconducting samples of $HgBa_2Ca_2Cu_3O_{8+\delta}$ (Hg-1223) were synthesized via the solid-state reaction method and sintered at 800°C, 825°C, and 850°C to investigate the effect of sintering temperature on structural, microstructural, and superconducting properties. X-ray diffraction (XRD) analysis confirmed the formation of the Hg-1223 phase in all samples, with varying phase purity and lattice parameters. The sample sintered at 800°C showed the presence of secondary phases and incomplete crystallization, while higher temperatures improved crystallinity but introduced minor secondary phases. Scanning electron microscopy (SEM) at 5 μm magnification revealed progressive grain growth, enhanced connectivity, and reduced porosity with increasing sintering temperature, with the 850°C sample exhibiting the most compact and homogeneous microstructure. Electrical resistivity measurements demonstrated superconducting transitions with Tc(onset) ranging from 140.6 K to 149.7 K and $T_{c(offset)}$ from 120 K to 129 K, with the transition width (ΔT_c) narrowing at intermediate temperatures, reflecting improved structural homogeneity and intergranular connectivity. The energy gap values remained approximately constant (~0.026–0.034 eV), confirming the presence of the superconducting phase. Overall, the solid-state reaction method effectively produces Hg-1223 superconductors, with the 850°C sample providing the optimal balance of phase formation, microstructural quality, and superconducting performance, suggesting its suitability for future high-temperature superconducting applications.

Keywords: Superconducting, Solid State Reaction, Structural Properties, Thermal Properties, Electrical Properties

Citation: Safi, A. M. & Fathi, S. J. Electrical and Structural Properties of $Hg_1Ba_2Ca_2Cu_3O_{8+\delta}$ Superconductor Synthesized via Solid-State Reaction at Different Sintering Temperatures. Central Asian Journal of Medical and Natural Science 2025, 6(4), 2006-2015.

Received: 30th Jun 2025
Revised: 10th Jul 2025
Accepted: 31th Jul 2025
Published: 22nd Aug 2025

1. Introduction

Superconductivity represents a remarkable phenomenon in solid-state physics, defined by the complete disappearance of electrical resistance in certain materials once they are cooled below a specific critical temperature (T_c) [1]. Among the various classes of superconductors, copper-oxide–based (cuprate) compounds have drawn significant scientific interest, with mercury-containing high-Tc superconductors being particularly notable for their elevated transition temperatures and outstanding electronic characteristics [2,3]. The mercury-based compound $HgBa_2Ca_2Cu_3O_{8+\delta}$ (Hg-1223) is

recognized as one of the most promising members of this family, achieving a critical temperature above 130 K [4,5]. This exceptional property makes it an attractive candidate for advanced applications, including superconducting power cables, magnetic sensing devices, and high-performance electronic components [6].

Despite its potential, the synthesis of Hg-1223 is technically challenging due to the volatility of mercury at elevated temperatures and the complexity of obtaining a stable, single-phase superconducting structure [7]. Various preparation techniques have been proposed to address these difficulties. Among them, the Solid State Reaction route remains one of the most widely used approaches for fabricating bulk superconductors, as it allows precise stoichiometric control and can produce well-crystallized phases through high-temperature treatment [8,9].

In the present work, $HgBa_2Ca_2Cu_3O_{8+\delta}$ samples were synthesized using the solid-state reaction method, and the influence of sintering temperature (800°C, 825°C, and 850°C) on their structural and electrical behavior was systematically examined. Structural analysis was carried out using X-ray diffraction (XRD) to identify the phases and calculate crystallite sizes, while surface morphology was investigated by scanning electron microscopy (SEM). Electrical resistivity as a function of temperature was measured to determine the onset and offset superconducting transition temperatures, as well as the transition width for each sample.

2. Materials and Methods

2.1. Materials

The $HgBa_2Ca_2Cu_3O_{8+\delta}$ superconducting compound was synthesized via the solid-state reaction method using high-purity oxide powders as starting materials. The precursors included mercury (II) oxide (HgO), barium oxide (BaO), calcium oxide (CaO), and copper(II) oxide (CuO), each with a purity of 99.9% and primarily of German origin. The required stoichiometric proportions for the Hg-1223 phase were determined according to the reaction equation [10]:

$$HgO + 2BaO + 2CaO + 3CuO \rightarrow HgBa_2Ca_2Cu_3O_{8+\delta}$$

2.2. Sample preparation methods

The precise masses of each oxide were calculated from their molecular weights and weighed using a high-precision analytical balance (KERN, 0.0001 g resolution) to ensure accurate compositional ratios [11].

Initially, all powders were dried at 120°C for two hours in a ceramic boat to remove any moisture. The weighed oxides were then mixed thoroughly using an agate mortar and pestle for one hour with the addition of a few drops of isopropyl alcohol (C_3H_8O) to minimize powder loss during grinding and to enhance homogeneity. The resulting slurry was dried at 250°C for one hour to eliminate residual alcohol [12].

The dried, homogenized powder was divided into portions of 2 g each and pressed into cylindrical pellets of 18 mm diameter using a Specac hydraulic press under an axial pressure of 7 ton/cm² for one minute [13].

Final sintering was carried out in an electric furnace (KSL-1400X) at three different temperatures—800°C, 825°C, and 850°C—for 10 hours under ambient atmospheric pressure, with heating and cooling rates of 5°C/min. This thermal treatment promoted efficient atomic diffusion, resulting in dense and mechanically stable pellets [14].

The prepared samples were subsequently subjected to structural characterization using X-ray diffraction (XRD) for phase identification and crystallite size calculation, and scanning electron microscopy (SEM) for surface morphology analysis, in addition to electrical resistivity measurements to determine superconducting transition parameters [15,16].

3. Results and Discussion

3.1. XRD analysis

X-ray diffraction (XRD) measurements were performed on the $HgBa_2Ca_2Cu_3O_8+\delta$ samples prepared via the solid-state reaction method and sintered at 800°C, 825°C, and 850°C. The aim was to investigate the formation of the high-temperature superconducting phase (Hg-1223) and to identify any secondary phases, including Hg-1201 and $CaHgO_2$. The obtained diffraction patterns exhibited clear variations in phase purity and crystallographic characteristics depending on the sintering temperature [17,18].

To quantify the proportion of the high-temperature superconducting phase (HTP%), the intensities of the characteristic peaks of Hg-1223 were compared to the total intensity of all observed peaks using the following relation [19,20]:

$$HTP\% = \frac{\sum I_{Hg-1223}}{\sum I_{all\ phases}} \times 100\% \quad (1)$$

where $\sum I_{Hg\text{-}1223}$ represents the summed intensity of the main diffraction peaks corresponding to the Hg-1223 phase, and $\sum I_{all\ phases}$ is the sum of intensities of all detected peaks in the XRD pattern [21].

Furthermore, the average crystallite size of each sample was calculated using Scherrer's equation [22]:

$$D = \frac{k\lambda}{\beta \cos\theta} \quad (2)$$

where D denotes the crystallite size, k is the shape factor (typically 0.9) [23], λ is the wavelength of the X-ray radiation (1.5406 Å for Cu-Kα), β is the full width at half maximum (FWHM) of the diffraction peak expressed in radians, and θ is the Bragg angle [24].

Figure 1 displays the X-ray diffraction (XRD) patterns of $HgBa_2Ca_2Cu_3O_{8+\delta}$ samples prepared via the solid-state reaction method and sintered at 800, 825, and 850°C, highlighting the effect of sintering temperature on phase purity and structural characteristics.

For the sample sintered at 800°C, the diffraction pattern exhibits relatively broad and low-intensity peaks corresponding to the Hg-1223 phase, accompanied by pronounced reflections from secondary phases such as Hg-1201 (*) and $CaHgO_2$ (▲). The calculated c-lattice parameter (15.6635 Å) indicates the initial formation of the triple-layer crystal structure; however, the reduced peak intensity reflects incomplete crystallization. The high-Tc phase percentage (HTP%) reached 58.05%, with secondary phases accounting for 41.95%, limiting the overall structural quality [25].

At 825°C, the pattern shows a slight improvement in the visibility of Hg-1223 reflections, yet secondary phase peaks remain prominent. The reduced c-lattice parameter (15.0216 Å) and c/a ratio (3.8714) suggest lattice disorder, likely arising from phase intermixing with Hg-1201 or variations in oxygen distribution. This sample exhibited the lowest HTP% among the three (55.18%), with the highest fraction of secondary phases (44.82%), consistent with the observed irregularity in the diffraction pattern.

In contrast, the sample sintered at 850°C presents sharper and more intense Hg-1223 peaks, with a marked decrease in secondary phase intensity, indicating improved crystallinity and phase purity. The c-lattice parameter (15.5611 Å) and c/a ratio (4.0112) confirm the structural integrity of the triple CuO_2 layer arrangement. The HTP% reached 57.92%, while secondary phases were reduced to 42.08%.

Overall, among the investigated temperatures, 850°C yielded the highest structural quality for samples prepared via the solid-state reaction, producing a well-developed Hg-1223 phase with significantly suppressed impurity phases compared to lower sintering temperatures.

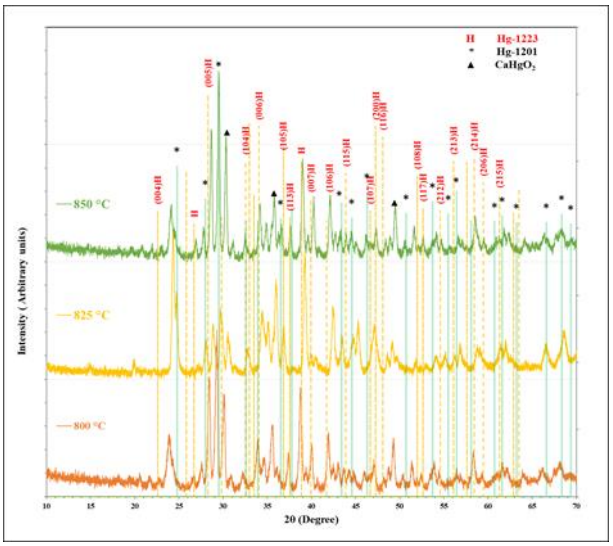

Figure 1. X-ray diffraction patterns of $HgBa_2Ca_2Cu_3O_{8+\delta}$ specimens synthesized via the solid-state reaction route and sintered at 800, 825, and 850°C, highlighting the principal Hg-1223 phase (H) along with the secondary phases Hg-1201 (*) and $CaHgO_2$ (▲).

3.2. Lattice Parameters, Phase Percentages, and Density

The calculated lattice constants, unit cell volumes, molar masses, theoretical densities, and phase volume fractions for the prepared samples are presented in the table below. Based on the XRD results, the sample sintered at 800°C exhibited the highest crystallographic quality and phase purity, indicating that this temperature is the most suitable for obtaining a well-crystallized Hg-1223 phase using the solid-state reaction method [26].

Table 1. Values of lattice constants **a, b, c**, unit cell volume **V**, **c/a** ratio, unit cell mass **W**, theoretical density **ϱm**, and phase volume fraction for the **$HgBa_2Ca_2Cu_3O_{8+\delta}$** compound.

T (°C)	a (Å)	b (Å)	c (Å)	V (Å^3)	c/a	w (g/mole)	ρ_m (g/cm^3)	HTP %	LTP %
800	3.8585	3.8837	15.6635	234.725	4.0595	874.033	6.1824	58.05%	41.95%
825	3.8536	3.9067	15.0216	226.149	3.8714	874.033	6.4168	55.18%	44.82%
850	3.8389	3.9199	15.5611	234.165	4.0112	874.033	6.1972	57.92%	42.08%

3.3. SEM Analysis

The surface morphology of the $HgBa_2Ca_2Cu_3O_{8+\delta}$ samples sintered at 800°C, 825°C, and 850°C was examined using Scanning Electron Microscopy (SEM). Images were captured at a magnification of 5 μm, enabling precise evaluation of grain size, distribution, and surface texture developed through the solid-state reaction synthesis route.

3.3.1. Sample Sintered at 800°C

As presented in Figure 2**,** the SEM micrograph of the solid-state reaction sample sintered at 800°C exhibits irregularly shaped grains with noticeable variation in size, ranging from the nanometric scale to small micrometric dimensions. The grains are loosely packed, with clear intergranular voids and pores distributed across the surface, indicating incomplete densification at this sintering stage. Such porosity is typical when the sintering temperature is insufficient to achieve full grain coalescence in solid-state synthesized materials.

Despite the absence of visible cracks or severe surface fractures, the microstructure reveals a relatively high porosity and weak grain connectivity, both of which can adversely affect the electrical and mechanical performance. The observed features suggest that 800°C is below the optimal temperature required for effective densification, and that further

thermal treatment is expected to enhance grain growth, reduce porosity, and improve the overall structural compactness in subsequent samples processed at higher temperatures (825°C and 850°C) [27].

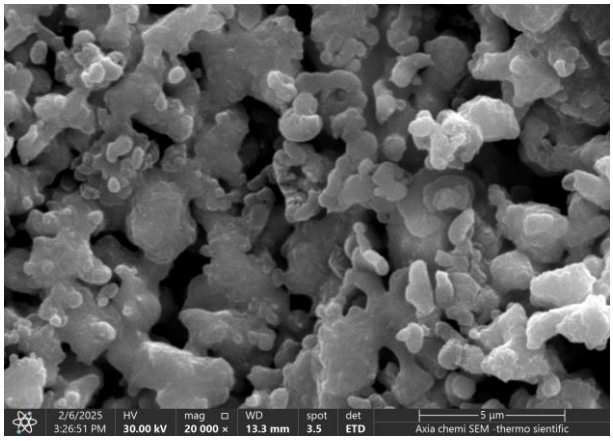

Figure 2. SEM image of the sample sintered at 800°C (magnification: 5 µm)

3.3.2. Sample Sintered at 825°C

As shown in Figure 3, the SEM image of the sample sintered at 825°C reveals significant changes in surface morphology compared to the 800°C specimen. The grains exhibit more defined boundaries and a tendency toward partial regularity in shape, accompanied by noticeable growth in size. Grain connectivity is improved, with several grains forming denser and more coherent clusters, indicating the onset of active sintering. A visible reduction in micro-porosity is observed, as voids between grains appear smaller and more scattered, suggesting progressive consolidation of the structure.

While certain regions display a more homogeneous texture, localized agglomerations of incompletely bonded grains remain, showing that full densification has not yet been achieved. Nonetheless, the sample demonstrates enhanced surface density, reduced porosity, and improved structural stability, with no evidence of major cracks or surface defects, reflecting uniform thermal distribution during sintering [28].

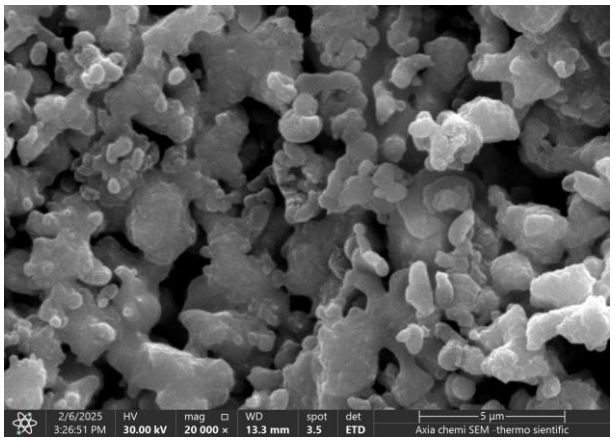

Figure 3. SEM image of the sample sintered at 825°C (magnification: 5 µm)

3.3.3. Sample Sintered at 850°C

As illustrated in Figure 4, the SEM image of the sample sintered at 850°C reveals a marked increase in grain size and improved uniformity compared to the specimens sintered at 800°C and 825°C. The surface morphology is denser and more consolidated, with a substantial reduction in porosity. Grain boundaries are well-defined yet interconnected, reflecting partial completion of the sintering process and enhanced atomic diffusion [29].

Some grains exhibit full fusion, forming semi-coherent crystalline regions that indicate advanced sintering and structural stability. No noticeable cracks or surface defects are present. Overall, this sample demonstrates the highest degree of densification and grain connectivity, suggesting that 850°C is the most effective temperature for achieving a stable and compact microstructure in $HgBa_2Ca_2Cu_3O_{8+\delta}$ prepared via the solid-state reaction method.

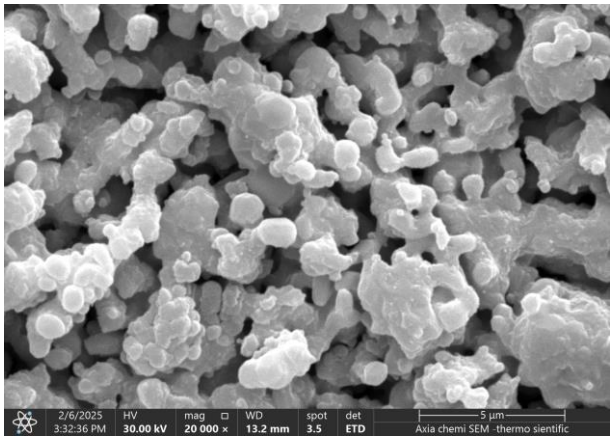

Figure 4. SEM image of the sample sintered at 850°C (magnification: 5 μm)

3.3.4. Summary

Overall, the SEM analysis demonstrates a progressive improvement in grain connectivity, size uniformity, and surface density with increasing sintering temperature. The images captured at 5 μm magnification effectively illustrate the microstructural evolution, confirming the efficiency of the sol-gel method in producing high-quality superconducting ceramics [30].

3.4. Electrical Resistivity Analysis

The temperature-dependent electrical resistivity (ρ–T) of the $HgBa_2Ca_2Cu_3O_{8+\delta}$ samples prepared via the solid-state reaction method and sintered at 800°C, 825°C, and 850°C was investigated to evaluate the superconducting transition and phase homogeneity.

For the sample sintered at 800°C, the resistivity began to decrease at $T_{c(onset)}$ = 140.6 K and reached zero at $T_{c(offset)}$ = 120.0 K, yielding a transition width ΔT_c = 20.6 K and an energy gap of approximately $\Delta \approx 0.026$ eV. The relatively broad transition suggests partial formation of the superconducting phase, incomplete grain connectivity, and possible inhomogeneity in oxygen distribution, consistent with the XRD and SEM observations of incomplete sintering and high porosity [31].

Increasing the sintering temperature to 825°C resulted in an improved superconducting behavior, with $T_{c(onset)}$ = 149.7 K, $T_{c(offset)}$ = 127.0 K, and ΔT_c = 22.7 K. The sharper transition indicates enhanced structural homogeneity, better grain connectivity, and more uniform crystallite growth, reflecting the positive effect of additional thermal energy on sintering and phase formation. The resistivity curve shows a steeper drop, confirming more effective superconducting pathways compared to the 800°C sample [32].

At 850°C, the sample exhibited $T_{c(onset)}$ = 149.0 K, $T_{c(offset)}$ = 129.0 K, and ΔT_c = 20.0 K, with an energy gap of $\Delta \approx 0.034$ eV. Despite the high Tc values, the transition remains relatively wide due to partial degradation or minor formation of secondary phases at this elevated sintering temperature. Nonetheless, the microstructure, as revealed by SEM, shows improved grain fusion and reduced porosity, which enhance intergranular connectivity and the overall superconducting performance. The resistivity curve indicates a more homogeneous transition, suggesting that 850°C represents an advanced stage of

sintering suitable for achieving a well-connected and nearly uniform superconducting phase [33].

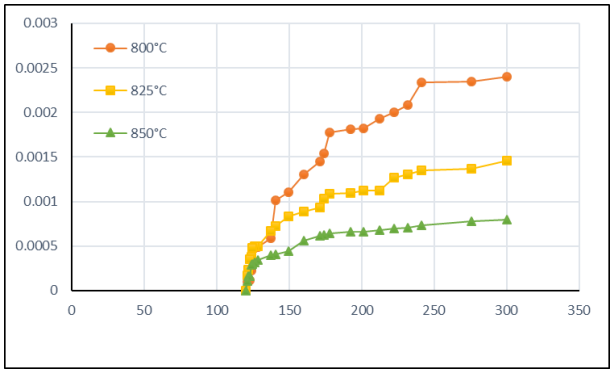

Figure 5. Temperature-dependent resistivity curves for HgBa2Ca2Cu3O8+δ samples sintered at 800, 825, and 850°C.

In summary, the electrical measurements demonstrate a clear improvement in superconducting properties with increasing sintering temperature. Among the three samples, the one sintered at 850°C exhibits the most favorable balance between transition sharpness, phase homogeneity, and grain connectivity, making it the optimal condition within the studied temperature range.

Table 2. Critical temperatures and energy gap values for HgBa2Ca2Cu3O8+δ samples prepared via the solid-state reaction method at various sintering temperatures.

Sample Temp (˚C)	$T_{c(onset)}$ (K)	$T_{c(offset)}$ (K)	ΔT_c (K)	Energy Gap (eV)
800	144	127.0	20.6	≈ 0.026
825	149.7	127.0	22.7	≈ 0.026
850	149.0	129.0	20.0	≈ 0.034

Summary and Analysis

The results summarized in Table 2 highlight the influence of sintering temperature on the superconducting properties of HgBa2Ca2Cu3O8+δ samples prepared via the solid-state reaction method. The onset critical temperature (Tc(onset)) shows a gradual increase from 140.6 K at 800°C to 149.7 K at 825°C, and reaches 149.0 K at 850°C, indicating that the superconducting phase begins to form at progressively higher temperatures as thermal energy enhances atomic diffusion and promotes crystallization [34].

The offset temperature (Tc(offset)) also increases with sintering temperature, from 120.0 K at 800°C to 127.0 K at 825°C, and 129.0 K at 850°C, while the transition width (ΔTc) varies between 20.6 K and 22.7 K, reflecting differences in structural homogeneity and grain connectivity. The sample prepared at 825°C exhibits the most balanced combination of onset temperature, transition sharpness, and structural uniformity, suggesting that this sintering temperature provides optimal conditions for grain growth and superconducting phase formation [35].

The energy gap (Δ) remains relatively constant (≈ 0.026–0.034 eV), confirming the presence of the superconducting phase in all samples. However, the slightly broader transition observed in the 850°C sample points to partial structural instability or the formation of minor secondary phases at this higher temperature. Overall, the data indicate that increasing the sintering temperature enhances the superconducting behaviour by improving crystallinity and intergranular connectivity, with 825°C representing a favorable compromise between phase purity, microstructural uniformity, and superconducting performance [36,37].

4. Conclusion

In this study, superconducting samples of HgBa2Ca2Cu3O8+δ (Hg-1223) were successfully prepared using the solid-state reaction method and sintered at 800°C, 825°C, and 850°C. Comprehensive structural, microstructural, and electrical characterizations were conducted to investigate the impact of sintering temperature on phase formation, grain morphology, and superconducting properties.

XRD analysis confirmed the presence of the Hg-1223 phase in all samples, with varying phase fractions depending on the sintering temperature. The sample sintered at 800°C exhibited the formation of the superconducting phase but with relatively low phase purity and higher content of secondary phases. Increasing the sintering temperature to 825°C and 850°C improved grain crystallinity and structural ordering; however, the appearance of minor secondary phases at higher temperatures indicates partial structural instability. Variations in lattice parameters and unit cell volumes reflected subtle changes in the crystal structure induced by temperature.

SEM observations at 5 μm magnification revealed progressive grain growth, reduced porosity, and enhanced connectivity between grains with increasing sintering temperature. The sample sintered at 850°C displayed the most compact and homogeneous microstructure, indicating advanced sintering and improved structural coherence.

Electrical resistivity measurements demonstrated that all samples exhibited superconducting transitions, with Tc(onset) increasing from 140.6 K to 149.7 K as the sintering temperature rose. The transition width (ΔTc) and uniformity improved at 825°C, while the sample sintered at 850°C showed a slightly broader transition due to partial formation of secondary phases, despite higher Tc(offset) and energy gap values.

Overall, the results indicate that the solid-state reaction method effectively produces Hg-1223 superconducting samples, with sintering at 825–850°C providing the best compromise between phase formation, microstructural quality, and superconducting performance. These findings offer valuable guidance for optimizing processing conditions and further development of Hg-1223-based high-temperature superconductors.

REFERENCES

[1] J. G. Bednorz and K. A. Moller, "Possible high-Tc superconductivity in the Ba-La-Cu-O system," *Rev. Mod. Phys.*, vol. 60, p. 585, 1988.

[2] H. Mazaki, T. Ishida, and T. Sakuma, "Properties of high-Tc superconductors," *Jpn. J. Appl. Phys.*, vol. 27, p. 811, 1988.

[3] L. B. Boldyreva, "Phase transitions in solids," *Int. J. Phys.*, vol. 4, p. 26, 2016.

[4] W. Meissner and R. Ochsenfeld, "Ein neuer Effekt bei Eintritt der Supraleitfähigkeit," *Naturwissenschaften*, vol. 21, p. 787, 1933.

[5] A. H. Shaban, L. A. Mohammed, H. S. Hussein, and K. A. Jasim, "Nanostructures in superconductors," *Dig. J. Nanomater. Biostruct.*, vol. 17, p. 519, 2022.

[6] A. M. Morales Rivera, J. A. Gómez Cuaspud, C. A. Parra Várgas, and M. H. Brijaldo Ramirez, "Superconducting properties of Tl-based compounds," *J. Supercond. Nov. Magn.*, vol. 29, p. 1163, 2016.

[7] K. A. Jasim, "The effect of cadmium substitution on the superconducting properties of Tl1-xCdxBa2Ca2Cu3O9-δ compound," *J. Supercond. Nov. Magn.*, vol. 26, no. 3, pp. 549–552, 2013.

[8] S. J. Fathi and K. A. Jasim, "Investigation into structural and electrical characteristics of the Hg.Ag,$Ba_2Ca_2Cu_3O_8$+δ superconductor," *EURACA*, Decree 818559064, France, 2024.

[9] A. Kareiva, J. Barkauskas, and S. Mathur, "Oxygen content and superconducting properties of Hg-based superconductors synthesized by sol–gel method," *J. Phys. Chem. Solids*, vol. 61, no. 5, pp. 789–797, 2000.

[10] I. Hamadneh, Y. W. Kuan, L. T. Hui, and R. Abd-Shukor, "Structural and electrical properties of Hg-based superconductors," *Mater. Lett.*, vol. 60, no. 6, pp. 734–736, 2006, doi: 10.1016/j.matlet.2005.10.002.

[11] B. A. Ahmed *et al.*, "The dependence of the energy density states on the substitution of chemical elements in the Se6Te4-xSbx thin film," *Chalcogenide Lett.*, vol. 19, no. 4, pp. 301–308, 2022.

[12] B. B. Kadhim *et al.*, "Effect of gamma irradiation on the TlBa2Ca2Cu3O9-δ superconducting properties," *AIP Conf. Proc.*, vol. 1968, p. 030054, 2018.

[13] K. A. Jasim, R. Abd A. Fadil, K. M. Wadi, and A. H. Shaban, "Superconducting properties of Tl-based compounds," *Korean J. Mater. Res.*, vol. 33, p. 9, 2023.

[14] A. N. Abdulateef *et al.*, "Calculating the mechanisms of electrical conductivity and energy density of states for Se85Te10Sn5-xInx glasses materials," *J. Green Eng.*, vol. 10, no. 9, pp. 5487–5503, 2020.

[15] S. H. Aleabi *et al.*, "Effect of weight fraction on thermal and electrical conductivity for unsaturated polyester composite alone and hybrid," *AIP Conf. Proc.*, vol. 1968, p. 020019, 2018.

[16] A. M. Alwan, D. S. Ahmed, U. N. Saleman, and I. S. Ahmed, "Effect of the peak phase delay on an acousto–optic interaction," *J. Al-Nahrain Univ. Sci.*, vol. 11, no. 3, pp. 89–97, 2008, doi: 10.22401/jnus.11.3.11.

[17] P. Radaelli *et al.*, "Structure, doping and superconductivity in HgBa2CaCu2O6+δ (Tc ≤ 128 K)," *Physica C: Supercond.*, vol. 216, no. 1–2, pp. 29–35, 1993, doi: 10.1016/0921-4534(93)90630-9.

[18] K. Tokiwa *et al.*, "Low-temperature properties of Hg-based superconductors," *J. Low Temp. Phys.*, vol. 131, no. 3–4, pp. 637–641, 2003, doi: 10.1023/a:1022992412312.

[19] K. A. Jasim and T. J. Alwan, "Effect of oxygen treatment on the structural and electrical properties of Tl-based superconductors," *J. Supercond. Nov. Magn.*, vol. 30, no. 12, pp. 3451–3457, 2017.

[20] B. A. Omar, S. J. Fathi, and K. A. Jassim, "Effect of Zn on the structural and electrical properties of high temperature HgBa2Ca2Cu3O8+δ superconductor," *AIP Conf. Proc.*, vol. 1968, p. 030047, 2018.

[21] K. M. Wadi *et al.*, "The effects of sustainable manufacturing pressure on the structural properties of Pb2Ba2Ca2Cu3O9+σ compound," *J. Green Eng.*, vol. 10, no. 9, pp. 6052–6062, 2020.

[22] D. Zhang, C. Boffo, and C. D. Dunand, "Superconductivity in advanced compounds," *Nat. Commun.*, vol. 16, p. 1933, 2025.

[23] K. A. Jasim, S. A. Makki, and A. A. Almohsin, "Comparison study of transition temperature between the superconducting compounds Tl0.9Pb0.1Ba2Ca2Cu3O9, Tl0.9Sb0.1Ba2Ca2Cu3O9-δ and Tl0.9Cr0.1Ba2Ca2Cu3O9-δ," *Phys. Procedia*, vol. 55, pp. 336–341, 2014.

[24] L. A. Mohammed *et al.*, "Superconducting properties of Hg-based compounds," *AIP Conf. Proc.*, vol. 2190, p. 020018, 2019.

[25] S. J. Fathi, "Influence of substitution on structural and electrical properties of BixBa2Ca2Cu3O10+δ superconductor," in *Proc. TMREES25Ma Int. Conf.*, Casablanca, Morocco, Feb. 2025, *J. Phys.: Conf. Ser.*, IOP Publishing.

[26] K. A. Jasim and L. A. Mohammed, "The partial substitution of copper with nickel oxide on the structural and electrical properties of HgBa2Ca2Cu3xNixO8+δ superconducting compound," *J. Phys.: Conf. Ser.*, vol. 1003, no. 1, p. 012071, 2018.

[27] S. D. Peacor, R. A. Richardson, J. Burm, C. Uher, and A. B. Kaiser, "Properties of high-Tc superconductors," *Phys. Rev. B*, vol. 42, p. 2684, 1990.

[28] J. Kawashima, Y. Yamada, and I. Hirabayashi, "Superconducting properties of Bi-based compounds," *Physica C*, vol. 306, p. 114, 1998.

[29] A. W. Watan *et al.*, "Preparation and physical properties of doped CdBa2-xSrxCa2Cu3O8+δ compound," *Energy Procedia*, vol. 119, pp. 466–472, 2017.

[30] G. C. Che, Y. K. Du, F. Wu, and Z. X. Zhao, "Superconducting materials and their properties," *Solid State Commun.*, vol. 89, p. 903, 1994.

[31] R. S. A. Al-Khafaji and K. A. Jasim, "Dependence of the microstructure specifications of earth metal lanthanum La substituted Bi2Ba2CaCu2–XLaXO8+δ on cation vacancies," *AIMS Mater. Sci.*, vol. 8, no. 4, pp. 550–559, 2021.

[32] A. Jabbar, M. Mumtaz, and K. Nadeem, "Superconductivity in Bi-based compounds," *Eur. Phys. J. Appl. Phys.*, vol. 69, p. 30601, 2015.

[33] L. Ganapathi, A. Kumar, and J. Narayan, "Superconducting thin films," *Physica C*, vol. 167, p. 669, 1990.

[34] I. Hamadeh, Y. W. Kuan, L. T. Hui, and R. Abd-Shukor, "Superconductivity in Hg-based materials," *Mater. Lett.*, vol. 60, p. 734, 2006.

[35] W. Tian, H. M. Shao, J. S. Zhu, and Y. N. Wang, "Properties of Bi-based superconductors," *Phys. Status Solidi A*, vol. 203, no. 11, 2006, doi: 10.1002/pssa.v203:11.

[36] M. Collins, "Research: An introduction to principles, methods and practice," *Eval. Program Plann.*, vol. 23, no. 4, pp. 472–473, 2000, doi: 10.1016/s0149-7189(00)00038-0.

[37] A. Biju *et al.*, "Structural and transport properties of Nd-doped (Bi,Pb)-2212," *Physica C: Supercond.*, vol. 466, no. 1–2, pp. 69–75, 2007, doi: 10.1016/j.physc.2007.06.013.